Nonequilibrium phase separation in traffic flows

Hisao Hayakawa*[1] and Ken Nakanishi†[2]

[1]: *Graduate School of Human and Environmental Studies, Kyoto University, Kyoto 606-01, Japan*

[2]: *Department of Mechanical Engineering, Shizuoka University, Hamamatsu 432, Japan*

arXiv:patt-sol/9707002v1 8 Jul 1997

Abstract

Traffic jam in an optimal velocity model with the backward reference function is analyzed. An analytic scaling solution is presented near the critical point of the phase separation. The validity of the solution has been confirmed from the comparison with the simulation of the model.

Typeset using REVTEX

*e-mail: hisao@phys.h.kyoto-u.ac.jp

†e-mail: tmknaka@eng.shizuoka.ac.jp

Recently, the importance of cooperative behavior in dissipative systems consisting of discrete elements has been recognized among physists. As a result, granular materials have been studied extensively from physical point of views. [1]. Similarly, to know the properties of traffic jams in daily life is also an attractive subject not only for engineers but also physists [2]. There are some similarities between two phenomena in particular in the simplest situation where cars and particles are respectively confined in a highway and a long tube. Thus, it is interesting to clarify common and universal mathematical structure behind these phenomena.

We propose here a model of the traffic flow

$$\ddot{x}_n = a[U(x_{n+1} - x_n)V(x_n - x_{n-1}) - \dot{x}_n], \tag{1}$$

where x_n and a are the positions of n th car, and the sensitivity, respectively. This model contains the psychological effect of drivers. Namely, the driver of x_n takes care of not only the distance ahead $x_{n+1} - x_n$ but also the backward distance $x_n - x_{n-1}$. The optimal velocity function U should be a monotonic increasing function of the distance of $x_{n+1} - x_n$ and $V - 1$ should be a monotonic decreasing function of $x_n - x_{n-1}$. Thus, we adopt

$$U(h) = \tanh(h-2) + \tanh(2); \quad V(h) = 1 + f_0(1 - \tanh(h-2)) \tag{2}$$

for the later explicit calculation. We put these optimal velocity functions as the product form UV in (1), because the driver of x_n cannot accelerate the car without enough the forward distance $x_{n+1} - x_n$ even when the distance $x_n - x_{n-1}$ becomes short. This model (1) with (2) is the generalization of the optimal velocity (OV) model proposed by Bando et al. [3]

$$\ddot{x}_n = a[U(x_{n+1} - x_n) - \dot{x}_n]. \tag{3}$$

Our model is also similar to the model of granular flow in a one dimensional tube

$$\ddot{x}_n = \zeta[\tilde{U}(x_{n+1} - x_{n-1}) - \dot{x}_n] + g(x_{n+1} - x_n) - g(x_n - x_{n-1}) \tag{4}$$

where the explicit forms of $\tilde{U}$ and the force g are not important in out argument. Although real systems contain variety of cars and particles and higher dimensional effects, we believe that the most essential parts of both traffic flows and granular pipe flows can be understood by pure one dimensional models (1) and (4). The reason is as follows: It is known [4] that model (4) supplemented by the white noise produces a power law in the frequency spectrum of the density correlation function $S(q,\omega) \sim \omega^{-4/3}$, whose exponent 4/3 is very close to the experimental value [4] and that by the lattice-gas automata simulation [5]. From this success the essential effects of randomness such as passing cars and variety of cars seem to be represented by the adding white noise to the models (1) and (4).

Komatsu and Sasa [6] reveal that the original OV model can be reduced into the modified Korteweg-de Vries (MKdV) equation at the critical point (the averaged car distance $h = 2$) for the phase separation. They also show that symmetric kink solitons deformed by dissipative corrections describe a bistable phase separation. The exactly solvable models in which the essential characteristics of the optimal velocity model are included have been proposed [7]. However, as will be shown, the generalized optimal velocity model (1) and granular model (4) as well as the fluid model of traffic flows by Kerner and Konhäuser [8] and two fluid models in granular flows [9] are not reduced to MKdV equation but exhibit the phase separations between a linearly unstable phase and a stable phase [10]. Thus, there is a wider universality class of dissipative particle dynamics which contains (1), (4) and fluid models [8,9].

The aim of this Letter is to obtain an analytic scaled solution of (1). To demonstrate quantitative validity of our analysis we will compare it with the result of our simulation. After the completion of our analysis on (1), we will briefly discuss the relation of the result and the expected results in (4) and fluid models.

Let us rewrite (1) as

$$\ddot{r}_n = a[U(h + r_{n+1})V(h + r_n) - U(h + r_n)V(h + r_{n-1}) - \dot{r}_n] \tag{5}$$

where h is the averaged distance of successive cars and r_n is $x_{n+1} - x_n - h$.

Now, let us consider the linear stability of (5). The linearized equation of (5) around $r_n(t) = 0$ is given by

$$\ddot{r}_n = a[U'(h)V(h)(r_{n+1} - r_n) + U(h)V'(h)(r_n - r_{n-1}) - \dot{r}_n] \tag{6}$$

where the prime refers to the differentiation with respect to the argument. With the aid of the Fourier transformation $r_q(t) = \frac{1}{N}\sum_{n=1}^{N} \exp[-iqnh] r_n(t)$ with $q = 2\pi m/Nh$ and the total number of cars N we can rewrite (6) as

$$(\partial_t - \sigma_+(q))(\partial_t - \sigma_-(q)) r_q(t) = 0 \tag{7}$$

with

$$\sigma_\pm(q) = -\frac{a}{2} \pm \sqrt{(a/2)^2 - aD_h[U,V](1 - \cos(qh)) + ia(UV)' \sin(qh)}, \tag{8}$$

where we drop the argument h in U and V. $D_h[U,V] \equiv U'(h)V(h) - U(h)V'(h)$ denotes Hirota's derivative. The solution of the initial value problem in (7) is the linear combination of terms in proportion to $\exp[\sigma_+(q)t]$ and $\exp[\sigma_-(q)t]$. The mode in proportion to $\exp[\sigma_-(q)t]$ can be interpreted as the fast decaying mode, while the term in proportion to $\exp[\sigma_+(q)t]$ is the slow and more important mode.

The violation of the linear stability of the uniform solution in (6) is equivalent to $Re[\sigma_+(q)] \geq 0$. Assuming $qh \neq 0$ ($qh = 0$ is the neutral mode), the instability condition is given by $2(UV)'^2 \cos^2(\frac{qh}{2}) \geq aD_h[U,V]$. Thus, the most unstable mode exists at $qh \to 0$ and the neutral curve for long wave instability is given by

$$a = a_n(h) \equiv \frac{2(UV)'^2}{D_h[U,V]}. \tag{9}$$

The neutral curve in the parameter space (a,h) is shown in Fig.1 for $f_0 = 1/(1 + \tanh(2))$ in (2). For later convenience, we write the explicit form of the long wave expansion of σ_+ in the vicinity of the neutral line

$$\sigma_+(q) = ic_0 qh - c_0^2 \frac{a - a_n(h)}{a_n(h)^2}(qh)^2 - i\frac{(qh)^3}{6}c_0 - \frac{(qh)^4}{4a_n(h)}c_0^2 + O((qh)^5) \tag{10}$$

where $c_0 = (UV)'$. Thus, the uniform state becomes unstable due to the negative diffusion constant appears for $a < a_n(h)$.

The simplest way to describe hydrodynamic mode is the long wave expansion. It is easy to derive the KdV equation near the neutral curve from (1) as in the case of fluid models [8,9]. To describe the phase separations, however, we should choose the critical point $(a, h) = (a_c, h_c)$ from the cross point of $(U(h)V(h))'' = 0$ where the coefficient of $\partial_x r^2$ becomes zero and the neutral curve, because KdV equation only has pulses while cubic nonlinear terms can produce the interface solution to connect two separated domains. The explicit critical point of (2) with $f_0 = 1/(1 + \tanh(2))$ is given by

$$h_c = 2 - \tanh^{-1}(1/3) \simeq 1.65343; \quad a_c = \frac{512}{81} f_0^2 \simeq 1.63866. \tag{11}$$

Unfortunately, the reduced equation based on the long wave expansion of our model is an ill-posed equation. In fact, the scalings of variables as $r_n(t) = \epsilon r(z, \tau)$,$z = \epsilon(x + c_0 t)$ and $\tau = \epsilon^3 t$ with $\epsilon = \sqrt{(a_c - a)/a_c}$ leads to

$$\partial_\tau r = a_1 \partial_z r^3 - a_2 \partial_z^3 r + a_3 \partial_z^2 r^2 \tag{12}$$

in the lowest order, where a_1, a_2 and a_3 are constants. Its linearized equation around $r = d_0$ is unstable for all scale, because the solution with $r - d_0 \simeq \exp[ikz + \lambda_k \tau]$ has the growth rate $Re[\lambda_k] = 2k^2 a_3 d_0$ which is always positive when $a_3 d_0 > 0$.

Of course, this irregularity in the short scale is from the long wave approximation. The regularity of the original model (1) can be checked easily as follows: Let $x = nh$ be regarded as a continuous variable. From $r(x \pm h, t) = \exp[\pm h \partial_x] r(x, t)$ or the Fourier component $\exp[\pm iqh]$ of the translational operator $\exp[\pm h \partial_x]$, the function of the translational operation in the shortest scale ($qh = \pi$ in the Fourier space) is $r(x \pm h, t) \to -r(x, t)$. Thus, our model in (5) for $r(x, t)$ in the shortest scale is reduced to

$$\partial_t^2 r = a[W(r) - \partial_t r], \quad W(r) \equiv U(h - r)V(h + r) - U(h + r)V(h - r). \tag{13}$$

Substituting (2) into (13) it is easy to show $W'(r) = -(\mathrm{sech}^2(h - r - 2) + \mathrm{sech}^2(h + r -$

2))$\{1 + f_0(1 + \tanh(2))\} < 0$. Then, the growth rate of the linearized equation of (13) by $r - d_0 \sim \exp[\lambda t + ikx]$ is given by

$$\lambda = \frac{-a \pm \sqrt{a^2 - 4a|W'(d_0)|}}{2}, \tag{14}$$

where $Re[\lambda] \leq 0$ for any d_0. Thus, the original model (1) is stable for the perturbation in the short scale.

Although it is possible to derive a regularized long wave equation thanks to the Pade approximation [11], the result is more complicated than the original model (1). Thus, to obtain the asymmetric propagating kink solution, we only eliminate the fast decaying mode in (5) as

$$(\partial_t - \sigma_+(\partial_x))r(x,t) = (\sigma_+ - \sigma_-)^{-1} N[r(x,t)], \tag{15}$$

where $N[r]$ represents the nonlinear terms coming from UV. Since $(\sigma_+ - \sigma_-)^{-1}$ is the inverse of the polynomial of the differential operators, it is convenient to use the expansion $(\sigma_+ - \sigma_-)^{-1} \simeq a^{-1}[1 - \frac{2h}{a}(UV)'\partial_x + O(h^2)]$. Equation (15) is the regularized partial differential equation.

To obtain the scaled propagating kink solution we assume the scaling of the variables by $\epsilon = \sqrt{(a_c - a)/a_c}$ as

$$r(x,t) = \epsilon\sqrt{\frac{6c}{|(UV)'''|}} R(z), \quad z = \epsilon\sqrt{\frac{6c}{c_0}}(\frac{x}{h} + c_0 t - \epsilon^2 ct) \tag{16}$$

where the argument is fixed at $h = h_c$, and c is the positive free parameter which will be determined from the perturbation analysis. Substituting (16) into (15) and use the expansion

$$N[r]/a = \sum_{n=1}^{\infty}\sum_{m=2}^{\infty} h^m C_{mn}\partial_x^n r^m - h^3 U'V'\partial_x r\partial_x^2 r + \cdots \tag{17}$$

where $C_{21} = \frac{1}{2}(UV)'', C_{22} = \frac{1}{4}D_h[U,V]', C_{23} = \frac{1}{12}(UV)'', C_{31} = \frac{1}{6}(UV)''', C_{32} = \frac{1}{12}D_h[U,V]'', C_{41} = \frac{1}{24}(UV)''''$, and integrate by part of (15), we obtain

$$\frac{d^2R}{dz^2} - R(R^2 - 1) + \beta\frac{d}{dz}(R^2) = \epsilon\sqrt{\frac{c}{c_0}} M[R], \tag{18}$$

where $\beta = 3D_h[U,V]'/(2\sqrt{c_0|(UV)'''|})$. Here we neglect the contribution from the boundary and

$$M[R] = \rho_{23}\left(\frac{dR}{dz}\right)^2 - \rho_{32}\frac{dR^3}{dz} - \rho_{41}R^4 - \frac{1}{4\eta}(4\frac{dR}{dz} + \frac{d^3R}{dz^3} - 2\frac{c_0}{c}\frac{dR}{dz}), \tag{19}$$

where $1/\eta = \sqrt{6}D_h[U,V]/c_0$, , $\rho_{23} = 3\sqrt{6}U'V'/\sqrt{c_0|(UV)'''|}$, $\rho_{32} = \sqrt{3/2}D_h[U,V]''/|(UV)'''|$ and $\rho_{41} = \sqrt{3c_0}(UV)''''/(2\sqrt{2|(UV)'''|^3})$. Assuming $R(z) = R_0(z) + \epsilon R_1(z) + \cdots$, we obtain an asymmetric kink-antikink solution

$$R_0(z) = \tanh(\theta_\pm z); \quad \theta_\pm = \frac{\beta \pm \sqrt{\beta^2+2}}{2} \tag{20}$$

in the lowest order. The linearized equation of (20) can be reduced to

$$\mathcal{L}R_1 = \sqrt{\frac{c}{c_0}}M[R_0]; \quad \mathcal{L} = \frac{d^2}{dz^2} + 1 - 3R_0^2 + 2\beta(R_0\frac{d}{dz} + \frac{dR_0}{dz}). \tag{21}$$

The solvability condition to determine c is

$$(\Phi_0, M[R_0]) \equiv \int_{-\infty}^{\infty} dz\Phi_0 M[R_0] = 0, \tag{22}$$

where Φ_0 satisfies $\mathcal{L}^\dagger\Phi_0 = 0$. The explicit form of Φ_0 is given by

$$\Phi_0(z) = (\mathrm{sech}[\theta_\pm z])^{1/\theta_\pm^2}. \tag{23}$$

Thus, the solvability condition is reduced to

$$\frac{c_0}{c} = 2 + \theta_\pm^2\left(2 - 3\frac{I_2^{(\pm)}}{I_1^{(\pm)}}\right) + 2\eta[3\rho_{32}\left(1 - \frac{I_2^{(\pm)}}{I_1^{(\pm)}}\right) + \frac{\rho_{41}}{\theta_\pm}\left(\frac{I_0^{(\pm)}}{I_1^{(\pm)}} - 2 + \frac{I_2^{(\pm)}}{I_1^{(\pm)}}\right) - \rho_{23}\theta_\pm\frac{I_2^{(\pm)}}{I_1^{(\pm)}}] \tag{24}$$

where $I_n^{(\pm)} = \int_{-\infty}^{\infty} dx(\mathrm{sech}x)^{1/\theta_\pm^2+2n} = \sqrt{\pi}\dfrac{\Gamma(1/(2\theta_\pm^2)+n)}{\Gamma(1/(2\theta_\pm^2)+n+1/2)}$.

To obtain the explicit form we adopt $f_0 = 1/(1+\tanh(2))$ in (2). In this case the coefficients in (24) are reduced to $\rho_{23} = -3/2$, $\rho_{32} = -\beta$, $\rho_{41} = -1/4$, $\eta = 1/(4\beta)$ $c_0 = 2^6 f_0/3^3 = 1.20689$, and $\beta = 3\sqrt{3}/(8\sqrt{2}f_0) = 0.902037$. Thus, we obtain c as

$$c_+ = 0.62485945; \quad c_- = 0.82170040, \tag{25}$$

where $c_\pm$ are respectively the solution of (24) corresponding to $\theta_\pm$. Since there are two propagating velocities, the linearly stable region invades the unstable region if there are many domains in the system.

To check the validity of our analysis we perform the numerical simulation of (1) and (2) with $f_0 = 1/(1 + \tanh(2))$ under the periodic boundary condition. We adopt the classical fourth-order Runge-Kutta scheme. Since our purpose is the quantitative test of (20) and (25), the initial condition is restricted to the localized symmetric form $r_n = 18.7/N(\tanh(n - N/4) - \tanh(n - 3N/4) - 1)$ where N is the number of cars. Taking into account the scaling properties we perform the simulation for the set of parameters $(\epsilon, N) = (1/2, 32), (1/4, 64), (1/8, 128), (1/16, 256)$ until r_n relaxes to steady propagating states. Our result is plotted in Figs.1 and 2. Figure 1 displays points which have the maximum and the minimum values of successive car distance in each parameter set, and theoretical coexistence curve

$$a = a_c \left(1 - \frac{(h - h_c)^2}{A^2}\right); \quad A \equiv \sqrt{\frac{6\bar{c}}{|(UV)'''|}} = 1.15850495992, \tag{26}$$

where the agreement with each other is obvious. Notice we adopt $\bar{c} = (c_+ + c_-)/2$ as the traveling velocity, because the domain cannot move due to the finite size effect. From this figure we can see that one of the branches is in the linearly unstable region but the theoretical curve recovers the simulation result. Figure 2 demonstrates that the numerical result has a scaling solution which has an asymmetric kink-antikink pair. The linear combination of our theoretical curve (20) and (25) is plotted as the solid line by choosing the position of the kink and the antikink. Our theoretical curve agrees with simulation value without other fitting parameters. The quantitative discussion on the spreading process due to the finite $c_+ - c_-$ will be discussed elsewhere.

Let us comment on the universality class of traffic flows and granular pipe flows. All of models introduced here except for (3) have asymmetric kink-antikink pairs and qualitatively resemble behaviors with each other. Komatsu [10] has derived (12) as the long wave equation from the fluid model of traffic flow [8] which is equivalent to the two-fluid models in granular

flows. It is also easy to derive (12) from (4). In this sense, granular flows and traffic flows compose a universality class and our discussion here essentially can be used in any models for traffic flows and granular pipe flows. On the other hand, OV model in (3) is a special case of the above generalized models. For example, the models with $f_0 = 0$ in (2) and $g''(a_c) = 0$ in (4) are reduced to MKdV equation.

In conclusion, we obtain the analytic scaling solution of (1) and (2) which describes the phase separation between a linearly unstable phase and a stable phase. The accuracy and relevancy of the solution are confirmed by the direct simulation.

One of the authors (HH) thanks Ooshida, T. for fruitful discussion. This work is partially supported by Grant-in-Aid of Ministry of Education, Science and Culture of Japan (09740314).

REFERENCES

[1] H.M.Jaeger, S.R.Nagel and R.B.Behringer, Rev.Mod.Phys. **68**, 1259 (1996) and references therein.

[2] e.g. D.Helbing, Traffic Dynamics: New Physical Modeling Concepts (Springer, Berlin, 1997).

[3] M.Bando, K.Hasebe, A.Nakayama, A.Shibata and A.Sugiyama, Phys.Rev.E **51**, 1035 (1995).

[4] O.Moriyama, N.Kuroiwa, and M.Matsushita, and H.Hayakawa, in preparation.

[5] G.Peng and H.J.Herrmann, Phys.Rev.E **49**, 1796 (1994).

[6] T.S.Komatsu and S.Sasa, Phys.Rev. E **52**, 5597 (1995).

[7] Y.Sugiyama and H.Yamada, Phys.Rev. E (to be published): K. Nakanishi, K.Itoh, Y.Igarashi, and M. Bando, Phys.Rev. E (to be published).

[8] B.S.Kerner and P.Konhauser, Phys.Rev. E **48**, 2335 (1993). , D.A.Kurtze and D.C.Hong, Phys.Rev.E **52** 218 (1995).

[9] see, e.g. G.K.Batchelor, J.Fluid Mech. **193**, 75 (1988): M. F. Göz, Phys.Rev.E **52**,3697 (1995).

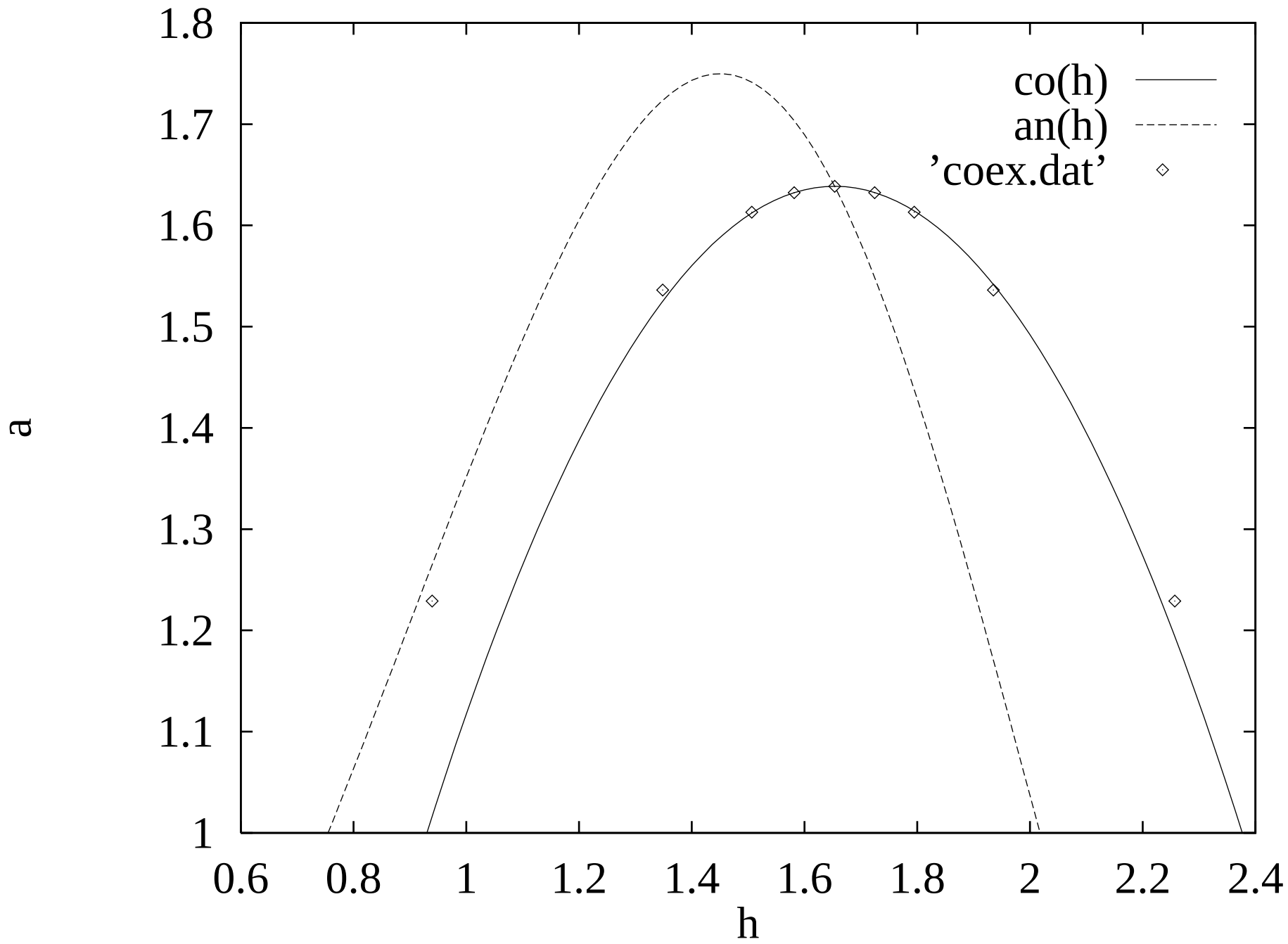
[10] T.S.Komatsu, PhD thesis (Tohoku University, 1996).

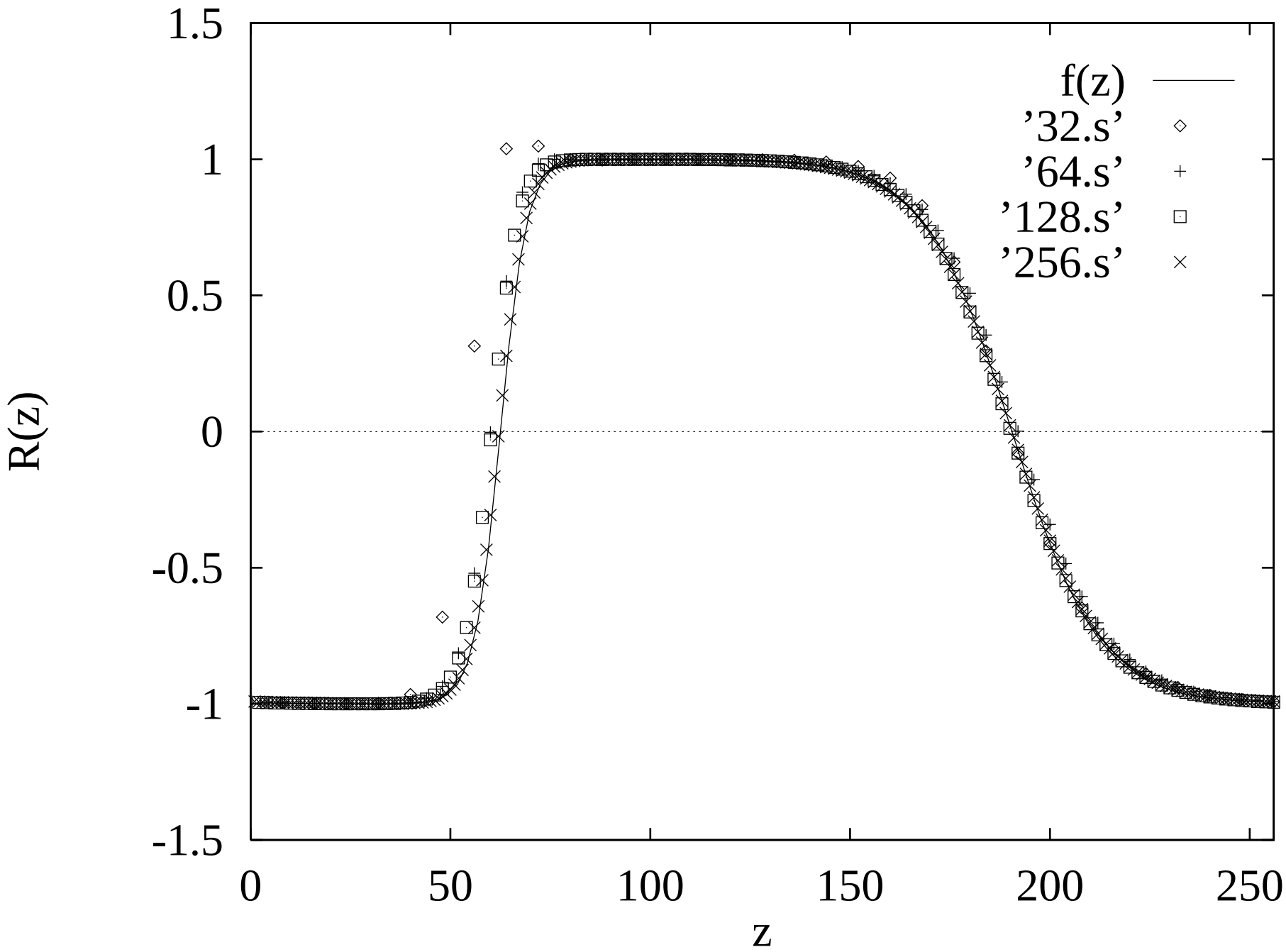
[11] Ooshida, T. and T. Kawahara, to appear in Phys. Rev. E.

FIGURES

FIG. 1. Plots of the coexistence curve (26), the solid line, and the neutral curve (9), the dashed line, as the functions of h. The scattered points are the maximum and the minimum distances of successive cars for a given a obtained from our simulation.

FIG. 2. The linear combination of our theoretical curve (20) and the scaled simulation data of the relative distance of succesive cars for $(\epsilon, N) = (1/2, 32), (1/4, 64), (1/8, 128), (1/16, 256)$, where $'N.s'$ denotes the scaled data for N cars systems. The solid curve is $f(z) = \tanh(\xi\theta_+(z - z_+)) - 1 + \tanh(\xi\theta_-(z - z_-))$ with $\xi = (6\bar{c}/c_0)^{1/2}/16 = 0.11851533$ and two fitting parameters $z_+ = 62.5$ and $z_- = 190.5$, where the spatial scale is measured by the average distance in $N = 256$.


co(h)
an(h)
'coex.dat'
a
h
1.8
1.7
1.6
1.5
1.4
1.3
1.2
1.1
1
0.6
0.8
1
1.2
1.4
1.6
1.8
2
2.2
2.4


1.5
1
0.5
0
-0.5
-1
-1.5
0
50
100
150
200
250
R(z)
z
f(z)
’32.s’
’64.s’
’128.s’
’256.s’